Korean Journal of Remote Sensing, Vol.26, No.3, 2010, pp.335~346

Development of an Efficient Processor for SIRAL SARIn Mode

Dong-Taek Lee*, Hyung-Sup Jung*†, and Geun-Won Yoon**

*Department of Geoinformatics, University of Seoul

**The third Technology Research Center, Agency for Defense Development

Abstract : Recently, ESA (European Space Agency) has launched CryoSAT-2 for polar ice observations. CryoSAT-2 is equipped with a SIRAL (SAR/interferometric radar altimeter), which is a high spatial resolution radar altimeter. Conventional altimeters cannot measure a precise three-dimensional ground position because of the large footprint diameter, while SIRAL altimeter system accomplishes a precise three-dimensional ground positioning by means of interferometric synthetic aperture radar technique. In this study, we developed an efficient SIRAL SARIn mode processing technique to measure a precise three-dimensional ground position. We first simulated SIRAL SARIn RAW data for the ideal target by assuming the flat Earth and linear flight track, and second accessed the precision of three-dimensional geopositioning achieved by the proposed algorithm. The proposed algorithm consists of 1) azimuth processing that determines the squint angle from Doppler centroid, and 2) range processing that estimates the look angle from interferometric phase. In the ideal case, the precisions of look and squint angles achieved by the proposed algorithm were about -2.0 μdeg and 98.0 μdeg, respectively, and the three-dimensional geopositioning accuracy was about 1.23 m, -0.02 m, and -0.30 m in X, Y and Z directions, respectively. This means that the SIRAL SARIn mode processing technique enables to measure the three-dimensional ground position with the precision of several meters.

Key Words : CryoSAT-2, SIRAL, SAR, Interferometry, Altimeter.

1. Introduction

Generally, a radar altimeter system has been used to measure altitude. It can accurately measure the altitude of sea level within several centimeters as well as prevent the crash of an aircraft on the ground by detecting the altitude during take-off and landing. The radar altimeter of TOPEX/Poseidon which finished its mission in 2006 measured the height of sea level with an accuracy of about 3.3 centimeters at an altitude of 1,366km (Ganachaud *et al.*, 1997). Its measurements provided useful information for marine activities by making it possible to understand thermal expansion and flow of seawater. However, as the radar altimeter measures only the distance between an aircraft and the Earth surface from the

Received June 15, 2010; Revised June 20, 2010; Accepted June 24, 2010.

† Corresponding Author: Hyung-Sup Jung (hsjung@uos.ac.kr)

travel time of a radio wave with a wide beam width of the altimeter, it is difficult to estimate an accurate land surface height from the radar altimeter.

On April 8th, 2010, the CryoSAT-2 satellite, which was launched by the ESA to investigate the glaciers of the Polar regions, was equipped with a new concept radar altimeter sensor named SIRAL (SAR/interferometric radar altimeter) which was developed by Thales Alenia Space. It has been known that the principle of the Poseidon altimeter made it possible not only to detect complicated topography such as the seashores of the North Pole, but also to measure the changes in the thickness of glaciers within centimeters (Wingham, 2002). In addition, SIRAL sensor has two remarkable characteristics in comparison to a radar altimeter. One is that operation modes differ according to the features of the Earth surface, and another is that high PRF of 17.8 kHz during a burst is used for SIRAL sensor. As to SIRAL, three modes of LRM (low resolution mode), SARM (synthetic aperture radar mode) and SARInM (synthetic aperture radar interferometric mode) are in operation (Rostan, *et al.*, 2001; Phalippou *et al.*, 2001). The LRM has the same principle to the radar altimeter, and SARM mainly is used to detect glaciers which have the characteristics of high reflectance but low backscattering by high surface scattering. The PRF (pulse repetition frequency) of the SARM is about 10 times higher than the LRM, and then the along-track resolution of the SARM is largely improved. The SARInM uses the interferometric phase obtained by two receivers. The look angle to LOS (line-of-sight) direction can be estimated from the phase difference between two antennas, and the accurate three-dimensional location is achieved by the estimated look angle (Rey *et al.*, 2001). As shown in Fig. 1, the signals returned from the closest ground surface are acquired by the two receivers simultaneously. The baseline between two

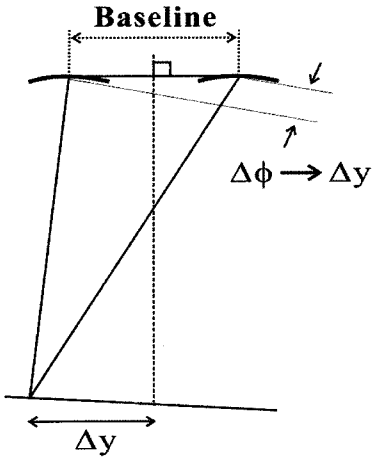

Fig. 1. Determination of across-track slant range distance from the phase difference (Raney, 2005).

sensors causes the phase difference ($\Delta\phi$) between two signals, and the across-track ground distance Δy can be calculated from this phase difference (Cullen, 2002). Another characteristic of the SIRAL sensor is to improve the along-track resolution largely. The SARM and SARInM modes transmit and receive 64 pulses in one burst with high PRF of 17.8 kHz (see Fig. 2). This high PRF of SARM and SARInM lead to the improved along-track resolution (Wingham *et al.*, 2006).

In this study, an efficient signal processing algorithm was proposed to measure a precise three-dimensional ground position from an interferometric radar altimeter, which is the SARIn mode of SIRAL sensor. This algorithm includes 1) range processing that determines the slant range distance from the range resolution improved by a chirp signal and that estimates the look angle from an interferometric phase, 2) azimuth processing that determines the squint angle from the Doppler centroid. This method enables to precisely measure the three-dimensional position of the nearest target from the RAW data of SIRAL SARIn mode that improves the azimuth and the range resolutions by using high PRF and SAR interferometry. To validate the performance of the

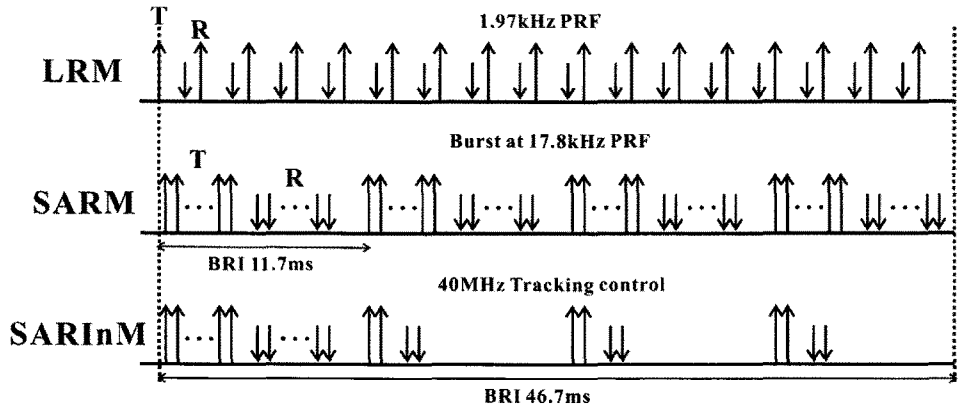

Fig. 2. SIRAL transmission and reception timing in the three measurement modes, where 'T' is trasmitted signal, 'R' is received signal, PRF is pulse repetition frequency, and BRI is burst repetition interval (Wingham *et al.*, 2006).

proposed method, we simulated the RAW signals returned from a point scatterer using the system parameters of the SIRAL SARIn mode, and analyzed the three-dimensional geopositioning accuracy achieved by the proposed algorithm.

2. CryoSAT-2 SIRAL Sensor SARIn Mode

As shown in Fig. 3, the SIRAL SARIn mode images the signal that arrives in a scatter of the shortest slant range distance during pulse duration. Bursts of 64 pulses at a PRF of 17.8 kHz with a burst repetition interval of 46.7 ms are transmitted. Because the pulses have to be correlated each other, the PRF within the burst is very high. Table 1 shows the system parameter of SIRAL SARIn mode.

According to the sampling theorem that it is necessary to sample the signal at a rate greater than twice its highest frequency component in order to recover the original signal, the sampling frequency of the received signal should be sufficiently larger than the chirp bandwidth. However, the sampling frequency of SIRAL SARIn mode is about 11.43 MHz, which is very smaller than the chirp bandwidth of about 350 MHz. This causes the phenomenon

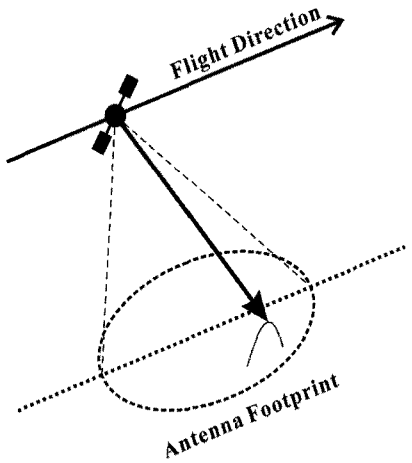

Fig. 3. Principle of data acquisition at point scatterer.

Table 1. System parameters of SIRAL SARIn mode

Parameters	Values
Chirp Duration Time (τ_p, μs)	44.8
FM Bandwidth (B, MHz)	350
Sampling Rate (t_s, μs)	0.0875
PRF (Hz)	17,800
Carrier Frequency (Hz)	13.575e+009
Effective Azimuth Antenna Dimension (m)	1.25
Effective Range Antenna Dimension (m)	1.13
Satellite Altitude (m)	717,000
Satellite Velocity (m/s)	7,000
Interferometer Baseline (m)	1.172

known as aliasing, which results in a frequency mistakenly taking on the identity of an entirely different frequency when recovered. The SIRAL SARIn mode overcomes this problem using the range gate time delay (τ_d) between azimuth lines. Fig. 4 represents the principle of the improvement of sampling frequency in SIRAL SARIn mode. As shown in Fig. 4(a), if the range gate time of the first azimuth line is τ, those of the second and the third azimuth lines will be $\tau + \tau_d$ and $\tau + 2\tau_d$, respectively. This time delay enables to recover the signals having the sampling frequency of more than 350MHz. Fig. 4(b) shows the rearranged range signal, where the (n,m) denote the pixel positions of azimuth and range, respectively.

The SIRAL SARIn mode images 64 pixels in azimuth direction and 512 pixels in range direction during a burst. From the first to the 32th azimuth lines, the range gate time increases by the range gate time delay whenever one azimuth line increases. That is, the thirty-two azimuth lines are acquired by using the different range gate times. The range gate time of the 33th azimuth line is equal to that of the first azimuth line, and the range gate time increases by the range gate time delay whenever one azimuth line increases. Consequently, we can obtain the rearranged RAW data of 2 pixels and 32×512 pixels from the SARIn RAW data of 64 pixels and 512 pixels in azimuth and range directions, respectively. This can improve the sampling frequency of SARIn mode by 32 times. The sampling frequency of about 11.43MHz in the original SARIn mode RAW data increases to about 365.76MHz in the rearranged RAW data. Because the improved sampling frequency is more than 350MHz which is the chirp bandwidth of SIRAL sensor, it is possible to mitigate largely the ghost phenomenon from the RAW data rearranged in range direction.

3. Data Processing

In order to develop and validate the signal processing method of SIRAL SARIn mode, the RAW data of an ideal scatterer is simulated using the system parameters of SIRAL SARIn mode. This method is composed of the range and azimuth processing to measure squint angle from Doppler centroid and look angle from interferometric phase. And then in the ideal case, the accuracy of three-dimensional geopositioning is analyzed. The azimuth processing consists of 1) zero-padding for the interpolation of Doppler power spectrum, 2) windowing for the smoothing of Doppler power spectrum, 3) FFT (fast fourier transform) in azimuth direction, 4) the multi-looking in range direction for

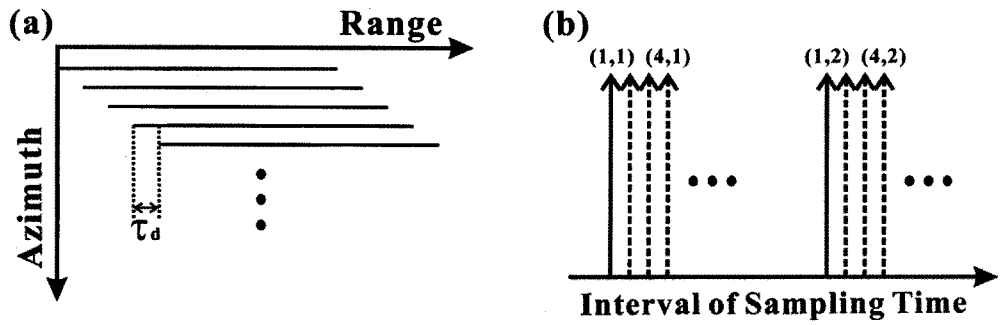

Fig. 4. Principle of the improvement of sampling frequency in CryoSAT-2 SIRAL SARIn mode: (a) the original SARIn RAW data and (b) the rearranged range data, where (n,m) represent the pixel positions of (azimuth, range), respectively, and τ_d is the range gate time delay.

the suppression of noises, 5) peak detection, and 6) the calculation of squint angle by estimating Doppler centroid from the measured peak positions. The procedures of the range processing include 1) the pixel rearrangement for the range compression, 2) the restoration of signals modulated by the range gate time delay, 3) windowing, 4) IFFT (inverse fast fourier transform) in range direction, 5) peak detection, 6) the multi-looking in azimuth, 7) the slant range distance determination, and 8) the measurement of look angle from the interferometric phase.

1) Generation of RAW Data

The RAW data of SIRAL SARIn mode is a complex image with 512 pixels in range direction and 64 pixels in azimuth direction. As mentioned above, the SIRAL SARIn mode only images the pulse that arrives fastest in the shortest slant range distance of a scatterer (see Fig. 3). In order to determine the accurate location of a scatterer, SARIn mode acquires the returned signals for 0.00340 seconds (64/PRF).

The SARIn mode uses high PRF of about 17,800Hz, while conventional SAR system images the data using PRF of approximately 2,000Hz. Moreover, a conventional SAR system compress the RAW data for a scatterer in azimuth direction for approximately one second, while SARIn mode of SIRAL sensor does not require the azimuth compression because it receives data just for the short time of about 0.00340 seconds.

The SARIn mode only needs to measure the squint angle in azimuth direction, and then calculate Doppler centroid for a scatterer in the Doppler frequency domain. In addition, in order to decrease the amount of data and simplify the procedure, the RAW data is sampled with the range gate time delay (τ_d) in azimuth direction (see Fig. 4).

After demodulation, the response from a point

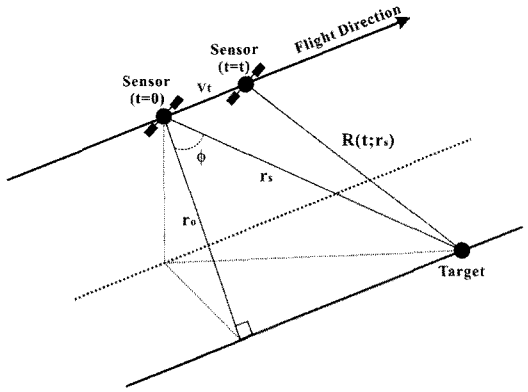

Fig. 5. SIRAL SARIn mode imaging geometry.

scatterer (Fig. 5) of SIRAL SARIn mode located at range r_s and at azimuth time $t = 0$ can be defined by (Davidson *et al.*, 1996; Raney *et al.*, 1994, Yeo *et al.*, 2001):

$$pp(\tau;r_s)=\sigma \cdot a(t;r_s) \cdot s_0\left[\tau-\frac{2R(t;r_s)}{c}\right] \cdot \exp\left[-i \cdot \frac{4\pi}{\lambda} \cdot R(t;r_s)\right] \quad (1)$$

where, τ is the delay time in the (slant) range direction, σ is the reflectivity of a scatterer, $a(t;r_s)$ is azimuth antenna weighting, λ is the radar wavelength and c is the speed of light, $R(t;r_s)$ is the time-varying distance from the radar to the scatterer and $s_0(\cdot)$ is the transmitted signal envelope. $R(t;r_s)$ can be defined as follows:

$$R(t;r_s) = \sqrt{V(r_s)^2t^2 + r_s^2 - 2r_sV(r_s)t\sin\gamma(r_s)} \quad (2)$$

where, $V(r_s)$ is the relative velocity proportionally parameter between the scatterer and the radar, and $\gamma(r_s)$ is the range dependent squint angle. And $s_0(\cdot)$ can be written by:

$$s_0\left[\tau-\frac{2R(t;r_s)}{c}\right] = \exp\left[ik\pi\left(\tau-\tau_d(t)-\frac{2R(t;r_s)}{c}\right)^2\right] \quad (3)$$

where, k means chirp modulation and τ_d the range gate time delay. Eq. (3) is expressed by the go-stop manner.

2) Measurement of squint angle from Doppler centroid

From Eq. (1), the phase of the range-compressed

signal $c(t;r_s)$ can be written by (Hein, 2004):

$$c(t;r_s) = \exp\left[-i\frac{4\pi}{\lambda}R(t;r_s)\right] \quad (4)$$

If approximating the slant range distance $R(t;r_s)$ by Taylor's series, Eq. (4) can be rewritten by:

$$c(t) \approx \exp\left[-i\frac{4\pi}{\lambda}r_s\right]\exp\left[i\cdot 2\pi\left(f_{DC}\cdot t - f_R\cdot\frac{t^2}{2}\right)\right] \quad (5)$$

where, f_{DC} is Doppler centroid and f_R is Doppler rate as given by:

$$f_{DC} = \frac{2V(r_s)\cdot\sin\gamma(r_s)}{\lambda} \quad (6)$$

$$f_R = \frac{2V^2(r_s)\cdot\cos^2\gamma(r_s)}{\lambda r_s} \quad (7)$$

The squint angle $\gamma(r_s)$ can be rewritten using the Doppler centroid from Eq. (6) as given by:

$$\gamma \approx \sin^{-1}\left[\frac{\lambda}{2V(r_s)}f_{DC}(r_s)\right] \quad (8)$$

Consequently, after the FFT in azimuth direction is applied to the range-compressed signal, the Doppler centroid is determined by detecting the peak from the Doppler power spectrum, and then the squint angle can be precisely calculated from the Doppler centroid using Eq. (8).

3) Measurement of look angle from radar interferometry

Fig. 6 compares a conventional radar altimeter with an interferometric SAR altimeter (SIRAL SARIn mode). A conventional radar altimeter measures the surface altitude using the signals returned from all ground targets within the beam width, while the interferometric radar altimeter estimates three-dimensional ground position by using the signals returned from a small area within the wide beam width. In conventional case, the height of flat surface can be measured precisely, but the height of land surface cannot be measured accurately because of topography. However, the interferometric radar altimeter improves the range resolution by 0.47 m using chirp pulse and the measurement accuracy of the LOS (line-of-sight) direction using the Doppler effect and the interferometric technique. As shown in Fig. 6(b), this altimeter system receives the transmitted signals from two sensors, and each of the two received signals is compressed by using the matched filtering, which is used for the conventional SAR compression. This compression step not only maximizes the range resolution but also enables to measure the accurate location of a scatterer in across-track direction using the interferometric phase of the two range-compressed signals.

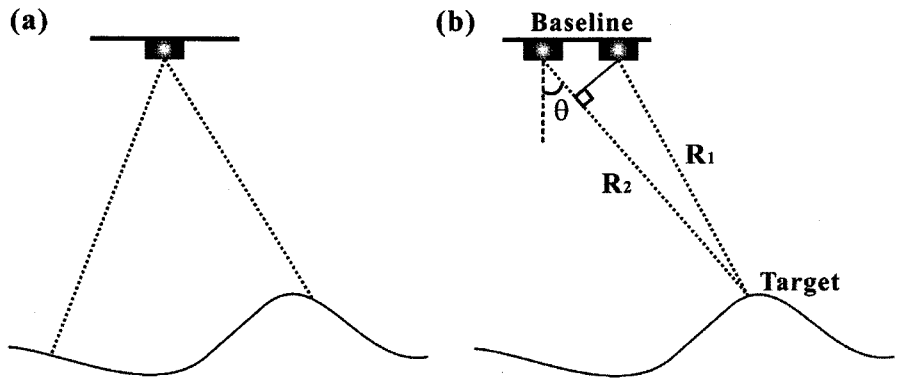

Fig. 6. Comparison of (a) conventional radar and (b) interferometric SAR altimeter systems. In the case of interferometric SAR altimeter, the improved positioning accuracy is achieved by interferometric SAR technique.

The look angle (θ) can be estimated by interferometric phase difference ($\Delta\phi$), which is calculated from the two range-compressed signals. The distances from the right and left antennas to the scatterer are R_1 and R_2, respectively (see Fig. 6(b)). The phases of left and right antennas are defined by:

$$\phi_1 = -\frac{4\pi}{\lambda} R_1 \tag{9}$$

$$\phi_2 = -\frac{2\pi}{\lambda}(R_1 + R_2) \tag{10}$$

The phase difference between the two antennas is defined by:

$$\Delta\phi = \phi_1 - \phi_2 = \frac{2\pi}{\lambda}(R_2 - R_1) \approx \frac{2\pi}{\lambda} B \sin\theta \tag{11}$$

where B is baseline length. From Eq. (11), the look angle can be defined by:

$$\theta = \sin^{-1}\left(\frac{\lambda}{2\pi} \cdot \frac{1}{B} \cdot \Delta\phi\right) \tag{12}$$

If the variation of the attitude of the satellite is considered (Fig. 7), the look angle can be redefined by the angle (α) between the baseline vector and horizontal plane vector as followed by:

$$\theta = \alpha + \sin^{-1}\left(\frac{\lambda}{2\pi} \cdot \frac{1}{B} \cdot \Delta\phi\right) \tag{13}$$

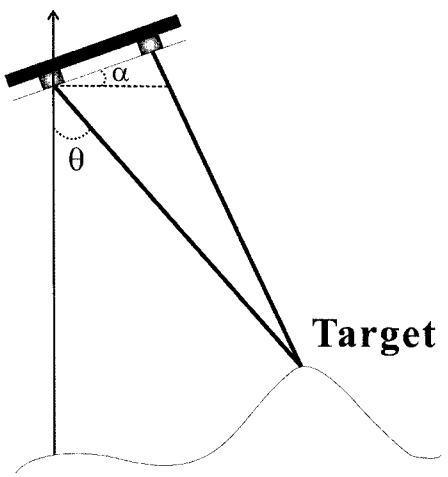

Fig. 7. Determination of look angle according to the variation of satellite's attitude.

Consequently, after finding the location of a scatterer from the range compressed signal, the look angle can be precisely measured from the estimation of the interferometric phase by detecting the target's pixel location using Eq. (13).

4) SARIn mode signal processing of SIRAL sensor

The efficient processing algorithm of SIRAL SARIn mode is developed in this study. Fig. 8 shows the block diagram of the proposed SIRAL SARIn mode processing. First, the return and reference signals are transformed into range frequency domain by FFT in range direction, and a complex conjugate multiplication is applied to FFT data of them. This step performs the range compression as well as compensates for the range gate time delay. The reference signal $s_r(\tau)$ can be defined using the chirp rate and the range gate time delay as given by:

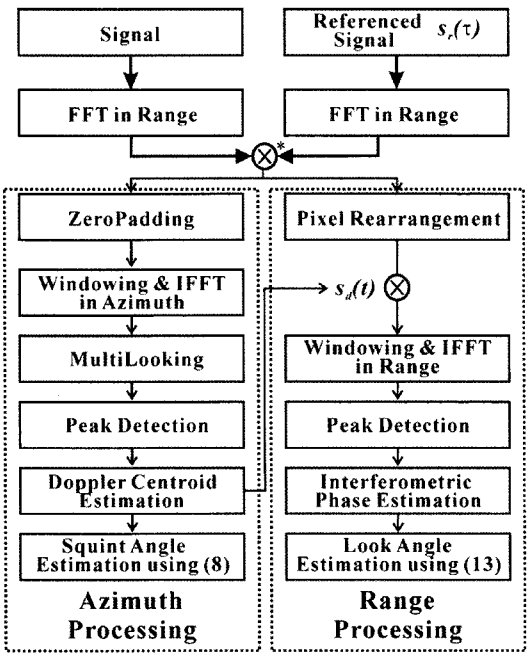

Fig. 8. Block diagram of the proposed SIRAL SARIn mode processing. The symbol * denotes a complex conjugate multiplication, and the number in brackets refers to the equation number in the main text.

$$s_r(\tau) = \exp\left[i \cdot 2\pi\left(k\tau_d\tau + \frac{k}{2}\tau^2\right)\right] \quad (14)$$

From the signals compressed in range direction and compensated for the range gate time delay, the squint and look angles and the slant range distance for the target can be measured through azimuth and range processing.

Azimuth processing is performed through the following procedures. In order to calculate the Doppler centroid accurately from the range compressed signal, the zero-padding is performed in azimuth direction, and Hanning window is applied for smoothing the Doppler spectrum in the frequency domain. And then the range compressed data is transformed into the Doppler frequency domain by FFT in azimuth direction. Because the Fourier transformed data normally contains noise, the range multi-look is applied. The Doppler centroid is extracted from the procedure of the peak detection, and the squint angle is calculated from the extracted Doppler centroid using Eq. (8). This azimuth processing does not perform azimuth compression unlike a conventional SAR compression, because the SIRAL SARIn mode does not require the azimuth compressed image but only the value of the Doppler centroid to estimate the squint angle of LOS direction. This decreases the azimuth processing time largely.

Range processing rearranges the range FFT data of the range-compressed signal in order to improve the range resolution, and compensates the azimuth frequency modulation caused by the change of slant range distance in along-track direction. The azimuth frequency modulation signal $s_d(t)$ can be defined as follows:

$$s_d(t) = \exp\left[-i \cdot 2\pi \cdot \left(f_{DC} \cdot t + \frac{1}{2} f_R \cdot t^2\right)\right] \quad (15)$$

Because the range FFT data is already compensated for the range gate time delay and multiplied by the FFT data of the reference signal, windowing is applied in order to decrease the side lobe effect, and then the IFFT in range direction is performed. After calculating the interferometric phase from the range compressed signals of right and left antennas, the slant range distance of a scatterer is measured by detecting the peak. A look angle is calculated by Eq. (13) from the interferometric phase. The range compression procedure of this range processing is performed in almost the same way to conventional SAR image compression. However, it is different from conventional SAR image in that the range processing of the SIRAL SARIn mode needs to compensate the azimuth frequency modulation and to rearranges the range FFT data for an efficient range compression. This does not only decrease the amount of data, but also the processing time.

As the above mentioned, the processing technique of interferometric radar altimeter for SIRAL SARIn mode can shorten the processing time because the azimuth compression is not performed, and can significantly decrease the amount of data using the rearrangement of the signals. This technique makes it possible to accurately measure the three-dimensional ground position of the Earth surface.

4. Simulation Results

To validate the proposed processing algorithm, 1) the RAW data of the ideal scatterer was simulated from system parameters of SIRAL SARIn mode, and 2) the accuracy of three-dimensional geopositioning was analyzed. For the simulation of SIRAL SARIn RAW data, the satellite's position was assumed as (0,0,H), and the position of three-dimensional point scatterer on the ground was determined from the squint and look angles using the imaging geometry

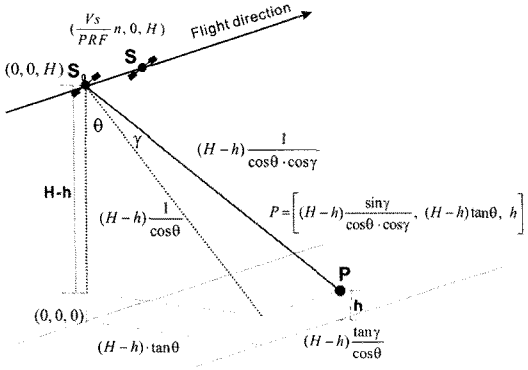

Fig. 9. Point scatterer geometry for SIRAL SARIn mode.

shown in Fig. 9. The simulation of the RAW data was performed on the assumptions 1) that the satellite's flight track is linear and 2) that the surface of the earth is flat. The satellite altitude is 717.2 km, the scatterer topographic height is 100.0 m, the squint and look angle were 0.5 deg which is used for the simulation respectively. The relative position of the ideal point scatterer was 6,258.64 m, 6,258.40 m and 100.00 m in X, Y and Z directions, respectively.

1) Simulation of RAW data

The RAW data of SIRAL SARIn mode is a complex image with 64 pixels in azimuth direction and 512 pixels in range direction, respectively. For the simulation of RAW data, we assumed that satellite's flight track is linear and the surface of the Earth is flat. The SIRAL SARIn mode images the signal that is returned from a scatter of the shortest slant range distance (Fig. 9). This system transmits and receives the chirp pulse for 0.0034 seconds, while the satellite moves about 25.2 m for the sampling interval of $\frac{V_s}{PRF} N_a$(V_s is the velocity of the satellite and N_a is the number of azimuth lines) in azimuth direction (see Table 1). And the RAW data is sampled with the range gate time delay in azimuth direction to decrease the amount of data and shorten the processing time. The sampling frequency should

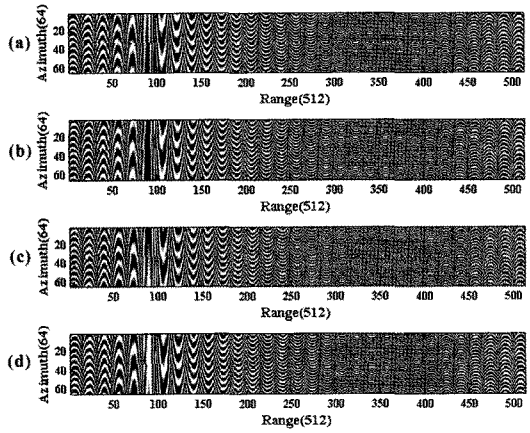

Fig. 10. (a-b) Represent the real and imaginary parts of the RAW data acquired from left antenna, and (c-d) right antenna.

be larger than the chirp bandwidth, but the SIRAL SARIn system has the sampling frequency of about 11.43 MHz, which is very smaller than the chirp bandwidth of 350 MHz. This problem is overcome by using the range gate time delay in azimuth direction (see Fig. 4). In this study, the RAW data of SIRAL SARIn mode was simulated on the basis of the characteristics of the SIRAL SARIn system and Fig. 10 shows the simulated SIRAL SARIn RAW data.

2) Estimation result of squint angle

The squint angle was estimated from the Doppler centroid for a scatterer in Doppler frequency domain. In order to estimate the squint angle, the zero-padding, the windowing, the FFT transform, the multi-looking in range direction, the peak detection and the calculation of the Doppler centroid were carried out. The Doppler centroid was determined by detecting the peak of the Doppler power spectrum. The interval of Doppler frequency is about 278 Hz, because the PRF of the SIRAL SARIn system is 17,800Hz and a number of azimuth lines is 64. This corresponds to the large squint angle of 25 mdeg. So, to improve the estimation of the Doppler centroid, the

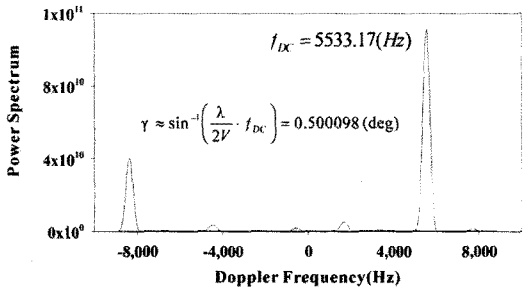

Fig. 11. Estimation of squint angle from Doppler centroid.

zero-padding of 1024 was applied in azimuth direction. In this ideal case, the true and estimated Doppler centroids were about 5533.17 Hz and 5532.09 Hz, respectively, and then the estimation error of the Doppler centroid was about 1.08 Hz. The error of the Doppler centroid corresponds to that of the squint angle of about 98 μdeg.

3) Estimation result of slant range distance and look angle

The look angle can be estimated by the interferometric phase, which is calculated from the two range-compressed signals by using matched filtering. After compensating the azimuth frequency modulation caused by the change of the slant range distance, the rearrangement of data was performed from 64 by 512 pixels to 2 by 16384 pixels in range and azimuth directions, respectively (see Fig. 4). The sampling frequency of the rearranged RAW data was improved by about 365.76 MHz and this is correspondent to spatial resolution of about 0.41 m. Because the improved sampling frequency was larger than chirp bandwidth, it was possible to compress the rearranged RAW data in range direction without the ghost phenomenon. The interferometric data was generated by a complex conjugate multiplication of the two range compressed signals and the position of point scatterer was determined by the peak detection. The estimated slant range distance from satellite to the point scatterer was about 717.197 km and the

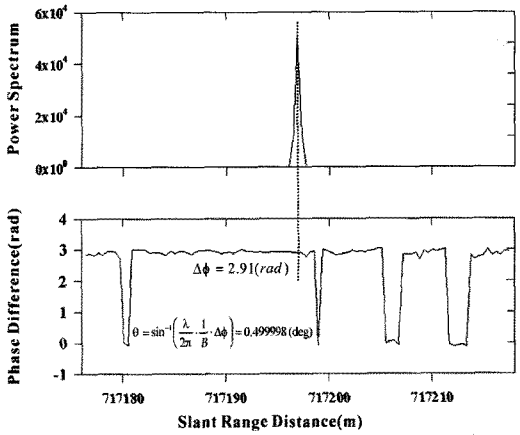

Fig. 12. Estimation of look angle from the interferometric phase.

interferometric phase difference was about 2.91 rad. The look angle estimated from the interferometric phase difference and true look angle was about 0.499998 deg and 0.5 deg, respectively, and the error of the look angle was about -2.0 μdeg (Fig. 12).

The errors of the squint angle, the look angle and slant range distance were 98.0 μdeg, -2.0 μdeg and 0.21 m, respectively. Because the estimated three-dimensional ground position were 6259.87 m, 6258.38 m, 99.70 m in X, Y and Z directions, respectively, the errors of 3D geopositioning were 1.23 m, -0.02 m and -0.30 m in X, Y and Z directions, respectively (see Table 2). This result means that the proposed method successfully can measure the three-dimensional ground position with the accuracy of several meters. However, the simulation was performed by ideal point scatterer. So,

Table 2. True and estimated values of squint and look angles and three-dimensional position of the simulated point scatterer

Parameters	True values	Estimated values	Errors
Squint angle (rad)	0.500000	0.500098	98.0e-006
Look angle (rad)	0.500000	0.499998	-2.0e-006
X-coordinate (m)	6258.64	6259.87	1.23
Y-coordinate (m)	6258.40	6258.38	-0.02
Z-coordinate (m)	100	99.70	-0.30

further study is required to consider the attitude of satellite, the height of the surface, the characteristics of the Earth surface, baseline decorrelation, etc.

5. Conclusion

The conventional radar altimeter system only measures the distance between surface and satellite from the travel times of a radio wave with a wide beam width of the altimeter, but CryoSAT-2 SIRAL SARIn system can estimate three-dimensional ground position within several meters using the radar interferometric technique. The characteristics of SIRAL SARIn sensor are 1) that it measures the accurate squint angle from Doppler centroid using high PRF of 17.8 kHz and 2) that it can estimate the accurate three-dimensional ground position using the interferometric radar method. The purpose of this study is to develop an efficient processing method of SIRAL SARIn mode. The proposed method is composed of 1) the azimuth processing to estimate the accurate squint angle and 2) the range processing to measure the look angle and the slant range distance. In the ideal case, the precisions of look and squint angles achieved by the proposed algorithm were about -2.0 μdeg and 98.0 μdeg, respectively, and the three-dimensional geopositioning accuracy was about 1.23 m, -0.02 m, and -0.30 m in X, Y and Z directions, respectively. This means that the SIRAL SARIn mode processing technique enables to measure the three-dimensional ground position with the precision of several meters.

Acknowledgements

This research was supported by Basic Science Research Program through the National Research Foundation of Korea(NRF) funded by the Ministry of Education, Science and Technology(2009-10132003) and researched by the supporting project to educate GIS experts.

References

Cullen, R. A. and Wingham, D. J., 2002, Cryosat Level 1b Processing Algorithms and Simulation Results, Proc. of 2002 International Geoscience and Remote Sensing Symposium, Toronto, Jun. 24-28, 2002. vol. 3, pp. 1762-1764.

Davidson, G. W., Cumming, I. G., and Ito, M. R., 1996. A Chirp Scaling Approach for Processing Squint Mode SAR Data, *IEEE Transactions on Aerospace and Electronic Systems*, 32(1): 121-133.

Ganachaud, A., Wunsch, C., M.-C., Kim, and Tapley, B., 1997. Combination of TOPEX/POSEIDON data with a hydrographic inversion for determination of the general circulation and its relation to geoid accuracy. *Geophysical Journal*, 128(3): 708-722.

Hein, A., Processing of SAR data, Springer, 2004.

Phalippou, L., Rey, L., and de Chateau-Thierry, P., 2001. Overview of the performances and tracking design of the SIRAL altimeter for the CryoSat mission, Proc. of 2001 International Geoscience and Remote Sensing Symposium, Sydney, Jul. 9-13, 2001. vol. 5, pp. 2025-2027.

Raney, R. K., 1998. The delay Doppler radar altimeter, *IEEE Transactions on Geosciences and Remote Sensing*, 36(5): 1578-1588.

Raney, R. K., Runge, H., Bamler, R., Cumming, I. G., and Wong, F. H., 1994. Precision SAR Processing Using Chirp Scaling, *IEEE*

Transactions on Geosciences and Remote Sensing, 32(4): 786-799.

Rey, L., de Chateau-Thierry, P., Phalippuo, L., Mavrocordatos, C., and Francis, R., 2001. SIRAL: a high spatial resolution radar altimeter for the Cryosat mission, Proc. of 2001 International Geoscience and Remote Sensing Symposium, Sydney, Jul. 9-13, 2001, vol. 7, pp. 3080-3082.

Rostan F. and Mallow, U., 2001. The CryoSat Earth Explorer Opportunity Mission-system calibration and mission performance, Proc. of 2001 International Geoscience and Remote Sensing Symposium, Sydney, Jul. 9-13, 2001, vol. 1, pp. 552-554.

Runge, H. and Bamler, R., 1992. A novel high precision SAR focusing algorithm based on chirp scaling, in Proc. IGARSS' 92, Houston, pp. 2385-2396.

Wingham, D. J., Cryosat: a mission to determine fluctuations in the Earth' s ice fields, Proc. of 2002 International Geoscience and Remote Sensing Symposium, Toronto, Jun. 24-28, 2002. vol. 3, pp. 1750-1752.

Wingham, D. J., Francis, C. R., Baker, S., Bouzinac, C., Brockley, D., Cullen, R., De Chateau-Thierry, P., Laxon, S. W., Mallow, U., Mavrocordatos, C., Phalippou, L., Ratier, G., Rey, L., Rostan, F., and Viau, P., Wallis, D.W., 2006. Cryosat: A mission to determine the fluctations in Earth's land and marine ice fields, *Advances in Space Research*, 37(4): 841-871.

Yeo T. S., Tan N. L., Zhang C. B., and Lu Y. H., 2001. A new subaperture approach to high squint SAR processing, *IEEE Transactions on Geosciences and Remote Sensing*, 39(5): 954-968.